

Liftoff and extinction characteristics of fuel- and air-stream-diluted methane–air flames

Andrew Lock^a, Alejandro M. Briones^a, Suresh K. Aggarwal^{a,*},
Ishwar K. Puri^b, Uday Hegde^c

^a Department of Mechanical and Industrial Engineering, University of Illinois at Chicago, Chicago, IL 60607, USA

^b Department of Engineering Science and Mechanics, Virginia Polytechnic Institute and State University, Blacksburg, VA 24061, USA

^c National Center for Microgravity Research, Cleveland, OH 44135, USA

Received 11 May 2006; received in revised form 20 February 2007; accepted 28 February 2007

Available online 23 April 2007

Abstract

Partial premixing of fuel and oxidizer is of common occurrence in fires. However, most previous studies dealing with flame extinction have focused on nonpremixed flames. In this experimental–numerical study, we examine the effectiveness of fuel-stream versus air-stream dilution for extinguishing laminar methane–air partially premixed (PPFs) and nonpremixed flames (NPF) using the chemically inert fire suppressant CO₂. Experimental measurements were made in lifted methane–air coflow flames, while both counterflow and coflow flames were simulated using a time-accurate implicit algorithm that incorporates detailed chemistry and includes radiation effects. Both measurements and simulations show that with fuel-stream dilution, PPFs stabilize at a higher liftoff height and blow out at a lower CO₂ dilution than NPFs. In contrast, with air-stream dilution, NPFs move to a higher liftoff height and blow out at a lower CO₂ dilution than PPFs. Despite different configurations, there is remarkable similarity in the extinction characteristics of coflow and counterflow flames with regard to the level of partial premixing and air- and fuel-stream dilution. The critical fuel-stream CO₂ mole fraction required for the extinction of both counterflow and coflow flames increases as ϕ is increased, i.e., as the level of partial premixing is reduced. Conversely, the critical air-stream CO₂ mole fraction decreases as ϕ is increased. Results also indicate a crossover value of $\phi \approx 2.0$, corresponding to the stoichiometric mixture fraction of $f_s = 0.5$, such that flames (including NPFs) with $f_s < 0.5$ are more difficult to extinguish with fuel-stream dilution, since oxygen is the deficient reactant, whereas flames with $f_s > 0.5$ are more difficult to extinguish with air-stream dilution, since fuel is the deficient reactant for these flames.

© 2007 The Combustion Institute. Published by Elsevier Inc. All rights reserved.

Keywords: Liftoff; Blowout; Extinction; Partially premixed; Laminar methane flames

1. Introduction

Flame extinction is important from both fundamental and practical considerations. Therefore, several analytical, numerical, and experimental investi-

* Corresponding author. Fax: +1 (312) 413 0441.
E-mail address: ska@uic.edu (S.K. Aggarwal).

gations have focused on the strain-induced extinction of counterflow nonpremixed (NPFs) and partially premixed flames (PPFs) [1,2]. The counterflow geometry is useful since it affords control over both the strain rate and the flame position [3]. In this context, the agent concentration requirements for the suppression of counterflow flames at low strain rates are also of interest, because they may correspond to the corresponding requirements for axisymmetric cup burner flames [4] that more closely represent real fire scenarios. However, most previous studies concerning flame extinction have characterized the air-stream agent requirements for the suppression of NPFs. There have been relatively few investigations on the fuel-stream agent requirements for the suppression of NPFs and PPFs, especially in a cup burner or coflow configuration.

Bundy et al. [5] investigated the fuel- and air-stream agent (N_2 , CO_2 , and CF_3Br) requirements for the suppression of low-strain-rate counterflow NPFs and observed that the air-stream-diluted NPFs extinguish at lower dilution than the corresponding fuel-stream diluted NPFs. Trees et al. [6] investigated the extinction of NPFs using a chemical agent, CF_3Br (Halon-1301), and surmised that the difference between the fuel- and air-stream effectiveness of a diluent could be attributed to preferential diffusion effects. Since their diluent was not chemically inert, it is not clear if the difference between the fuel- and air-stream effectiveness of inert agents (such as N_2 and CO_2) could also be attributed to such effects.

Flame extinction generally occurs due to three effects [7], namely, by reducing the (1) deficient reactant concentration so as to affect the reaction rates (dilution effect); (2) flame temperature (thermal effect), which decreases the radical pool; or (3) free radical concentration and thus interrupting the flame chemistry (chemical effect) by adding a chemical agent, such as halon. In this context, CO_2 , which is essentially chemically inert [8], can extinguish flames through both dilution and thermal effects. Halons have been successfully used as chemically active fire-suppression agents but have significant ozone depletion potential [9]. In addition, chemically active agents often generate substances in flames that prevent their use in occupied confined spaces. Therefore, CO_2 is considered in this investigation. It is also used as a fire-suppressant agent in the U.S. modules of the International Space Station.

There is a likelihood that unwanted fires can originate in a partially premixed mode when a pyrolyzed or evaporated fuel forms an initial fuel-rich mixture with the ambient air. It is often difficult to categorize such fires in terms of premixed flames or NPFs. In addition, catastrophic phenomena such as backdraft in building fires, which can have fatal conse-

quences [10–12], are also promoted by partially premixed combustion [13]. Hence, partially premixed combustion is an important consideration in the context of fire safety [14]. Moreover, previous studies have shown that the structure of PPFs can be modified significantly by changing the level of partial premixing [15]. Consequently, it is important to characterize the effectiveness of fuel-stream dilution versus air-stream dilution in extinguishing flames that are established at different levels of partial premixing. There is, however, relatively little fundamental information available in the literature on the extinction characteristics of PPFs, since most previous investigations have focused on the extinction of NPFs. Moreover, previous studies, except for one reported by Seiser et al. [16], have not examined the effectiveness of fuel-stream dilution versus air-stream dilution in extinguishing flames, especially in the context of PPFs.

Motivated by the above considerations, we report herein on an experimental and numerical investigation that examines the effectiveness of air-stream versus fuel-stream dilution in extinguishing nonpremixed and partially premixed flames. Lifted, laminar methane–air flames were established in axisymmetric coflowing jets, and the chemically inert diluent, CO_2 , was added either to the fuel stream or to the air stream. The diluent concentration was slowly increased until the lifted flame was extinguished (through blowout). For both air-stream and fuel-stream dilutions, the flame liftoff and blowout conditions were characterized for various levels of partial premixing in terms of the flame topology, liftoff height, and critical CO_2 mole fraction required for flame blowout. The CO_2 -diluted axisymmetric NPFs and PPFs were also simulated using a time-accurate, implicit algorithm that uses detailed descriptions of chemistry and transport. The computed flame topology, liftoff height, and critical CO_2 mole fractions when flame blowout occurred were compared with measurements. In addition, CO_2 -diluted NPFs and PPFs were simulated in a counterflow configuration and their extinction characteristics were investigated using various amounts of fuel- and air-stream dilutions. Here, our objective was to examine the similarity between the structures of coflow and counterflow flames at different dilution levels and the effect of geometry on their extinction characteristics.

It is important to distinguish between our study and that of Seiser et al. [16]. The cited study focused on the strain-induced extinction of PPFs in a counterflow configuration. In their case, the strain rate was continuously increased while keeping the equivalence ratio (ϕ) in one or both the streams fixed until the flame was extinguished. In contrast, we considered the dilution-induced extinction of lifted NPFs and PPFs in both coflow and counterflow configura-

tions in which the diluent mole fraction in the fuel (or air) stream was continuously increased until the flame extinguishment occurred through blowout. Moreover, Seiser et al. [16] obtained the critical strain rate as a function of ϕ while maintaining the adiabatic flame temperature and the stoichiometric mixture fraction at a constant value by appropriately controlling the amount of nitrogen in the two streams. Their purpose was to relate changes in the critical strain rate at extinction to changes in the level of partial premixing. In contrast, this investigation focuses on dilution-induced extinction at a fixed strain rate (in the case of counterflow flames) or a fixed flow time (coflow flames) so that the critical amount of CO₂ added to the fuel (or air) stream for flame extinction to occur can be related to the level of partial premixing. Consequently, the stoichiometric mixture fraction and adiabatic flame temperature are not held constant; indeed for this purpose they cannot be. In summary, in our investigation flame extinction is achieved by increasing the chemical time through dilution and thermal effects, while in the cited study, the extinction is achieved by decreasing the flow time.

2. Experimental methods

Laminar methane–air flames were established on a coannular burner with an inner diameter of 11.1 mm and an outer annulus diameter of 22.2 mm, shown in Fig. 1. The burner had several fine wire mesh inserts placed in the two ducts to facilitate a plug flow velocity profile. Both the fuel- and air-stream velocities were maintained at 0.5 m/s. The gas flow rates were controlled by MKS mass flow controllers, which are accurate to within 1% of their full scale. The fuel–air mixtures, as well as the diluents, were premixed

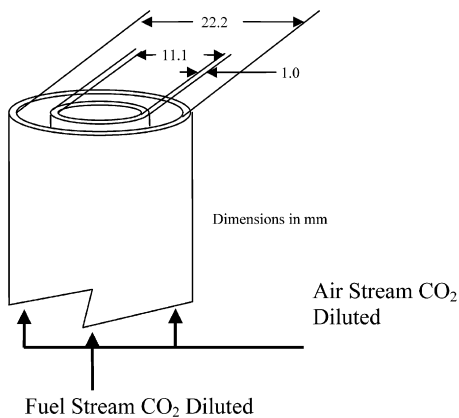


Fig. 1. Experimental burner used for experiments. Fine mesh screens are inserted into both annuli of the burner to have plug flow velocity profiles at the burner exit.

before each experiment in order to ensure consistent composition. The fuel–air–diluent mixtures are accurate to within 1% of the volumetric flow rate. The fuel-rich mixture was introduced through the inner duct and air through the outer annulus of the burner. The CO₂ diluent was introduced into the fuel stream or the air stream of the flame in order to compare the effectiveness of fuel- and air-stream dilution. The diluent concentration in either stream was varied to characterize flame liftoff and extinction (through flame blowout). Flame images were obtained using a digital camera (30 fps; 640 × 480 pixels) without using filters. The flames generally exhibited well-organized oscillations due to buoyant acceleration in normal gravity with oscillation frequencies in the range 10–15 Hz. Good agreement was observed between the simulated and experimental flame oscillation frequencies. A more detailed discussion of buoyancy-induced oscillations in partially premixed flames is presented elsewhere [17]. The flame liftoff height was determined by locating the displacement of the maximum chemiluminescence (representing the flame reaction kernel) from the burner rim. Experimental error in the measurement of liftoff height is limited by the resolution of the images. Generally, the measurement error is no more than ±10% of the values reported for liftoff height, L_f . The error is relatively small for flames stabilized near the burner (at lower L_f), but becomes more significant for flames near blowout.

3. Computational model

Axisymmetric coflow flames were simulated based on a computational model developed by Katta and co-workers [18,19]. The model solves the time-dependent governing equations for unsteady reacting flows in an axisymmetric configuration that can be written in a generalized form as

$$\begin{aligned} \frac{\partial(\rho\Phi)}{\partial t} + \frac{\partial(\rho v\Phi)}{\partial r} + \frac{\partial(\rho u\Phi)}{\partial z} \\ = \frac{\partial}{\partial r} \left(\Gamma^\Phi \frac{\partial\Phi}{\partial r} \right) + \frac{\partial}{\partial z} \left(\Gamma^\Phi \frac{\partial\Phi}{\partial z} \right) \\ - \frac{\rho v\Phi}{r} + \frac{\Gamma^\Phi}{r} \frac{\partial\Phi}{\partial r} + S^\Phi. \end{aligned} \quad (1)$$

Here t denotes the time, and u and v the axial (z) and radial (r) velocity components, respectively. The general form of the equation represents conservation of mass, momentum, species, or energy conservation, depending on the variable used for Φ . The diffusive transport coefficient Γ^Φ and source terms S^Φ are described in Ref. [18]. Introducing the overall species conservation equation and the state equation completes the equation set. A sink term based on an opti-

cally thin gas assumption was included in the energy equation to account for thermal radiation from the flame [20] in the form $q_{\text{rad}} = -4\sigma K_p(T^4 - T_0^4)$ [21] where T denotes the local flame temperature, and K_p accounts for the absorption and emission from the participating gaseous species (CO_2 , H_2O , CO , and CH_4) expressed as $K_p = P \sum_k X_i K_{p,i}$ where $K_{p,i}$ denotes the mean absorption coefficient of the k th species, σ is the Stefan–Boltzmann constant, and T_0 is the ambient temperature. The value of $K_{p,i}$ is obtained using a polynomial approximation to the experimental data provided in Ref. [21]. It should be noted that the optically thin radiation model does not account for the radiation absorbed by the added CO_2 in the fuel or air stream, which may lead to higher flame temperatures. However, previous investigations have shown that radiation absorption for CO_2 -diluted CH_4 -air flames becomes significant only at super-atmospheric pressures [22]. Although we expect that CO_2 absorption would slightly increase the flame temperature for all cases, our quantitative results in terms of the relative fuel- and air-stream effectiveness would remain the same. Moreover, since our flames are established at moderate and high global strain rates, the characteristic convection time is small in comparison with the radiation cooling time.

The thermodynamic and transport properties appearing in the governing equations are temperature- and species-dependent. The thermal conductivity and viscosity of the individual species were based on Chapman–Enskog collision theory, following which those of the mixture are determined using the Wilke semiempirical formulas [23]. Chapman–Enskog theory and the Lennard–Jones potentials were used to estimate the binary-diffusion coefficient between each species and nitrogen. The methane–air chemistry was modeled using a reduced mechanism following Peters [24]. This mechanism, designated as the C_2 mechanism, involves 24 species and 81 elementary reactions. The mechanism has been extensively validated previously for the computation of premixed flame speeds and the detailed structure of both NPFs and PPFs [18–20].

The computational domain consisted of 150×100 mm in the axial (z) and radial (r) directions, respectively, and contained a staggered, nonuniform (401×101) grid system. The minimum grid is ≈ 0.1 mm in both the z and r directions. The numerical experiments establishing the grid independence of the results have been reported elsewhere [25]. Both the inner and outer jets had uniform velocities of 50 cm/s. An isothermal insert simulates the inner 2×1 -mm burner wall at 300 K. The inner jet was assumed to issues a fuel–air mixture while the outer jet provided air. In lieu of quantitative flowfield data at the inlet boundary, every effort has been made to

create uniform experimental boundary conditions and match the inflow boundary conditions between experiments and simulations. This was accomplished by inserting fine mesh screens in the experimental burner to produce a nearly uniform flow profile at the burner exit and by tweaking the simulated burner exit velocity profile so that resulting predicted and measured flames matched as closely as possible. A detailed discussion of the boundary conditions is presented elsewhere [18,19]. Once undiluted flames were established, CO_2 was gradually added in the fuel stream or the air stream until blowout occurred [26].

Simulations of counterflow methane–air flames, established at various fuel-stream equivalence ratios, global strain rates, and fuel- and air-stream dilutions, were performed using the CHEMKIN package [27]. The flame chemistry was modeled using the GRI-Mech 3.0 mechanism [28]. It should be noted that while coflow flames are simulated using the (reduced) C_2 mechanism for computational efficiency, the counterflow flames, which are characterized by a one-dimensional flow field, are simulated using a detailed mechanism. The differences between the two mechanisms in terms of the critical CO_2 mole fraction for extinction are expected to be small. The distance between the two nozzles was 2.54 cm. The fuel and oxidizer temperatures were assumed to be 300 K. The grid independence of the results was achieved by controlling the values of the GRAD and CURV parameters, both of which were set at 0.1, using adaptive regridding in order to resolve the structures of both the premixed and nonpremixed reaction zones. Mixture-averaged transport properties were used for all simulations and little difference was observed in the simulations between mixture-averaged and multi-component transport.

4. Results and discussion

4.1. Validation of numerical model

The 2-D axisymmetric flame simulations have been previously validated against measurements for a variety of steady and unsteady flames, including opposed-jet diffusion flames [29], and burner-stabilized [19,30] and lifted jet flames [26]. Katta et al. [29] compared the predicted OH concentrations in opposed-jet flames with PLIF measurements that showed good agreement. Shu et al. [30] reported good agreement between the predicted and measured velocity fields (using PIV), and between the predicted heat-release-rate contours and the measured C_2^* -chemiluminescence images for methane–air PPFs. Likewise, Takahashi et al. [31] reported good agreement between the predicted and measured velocity fields using PIV for methane–air jet diffusion

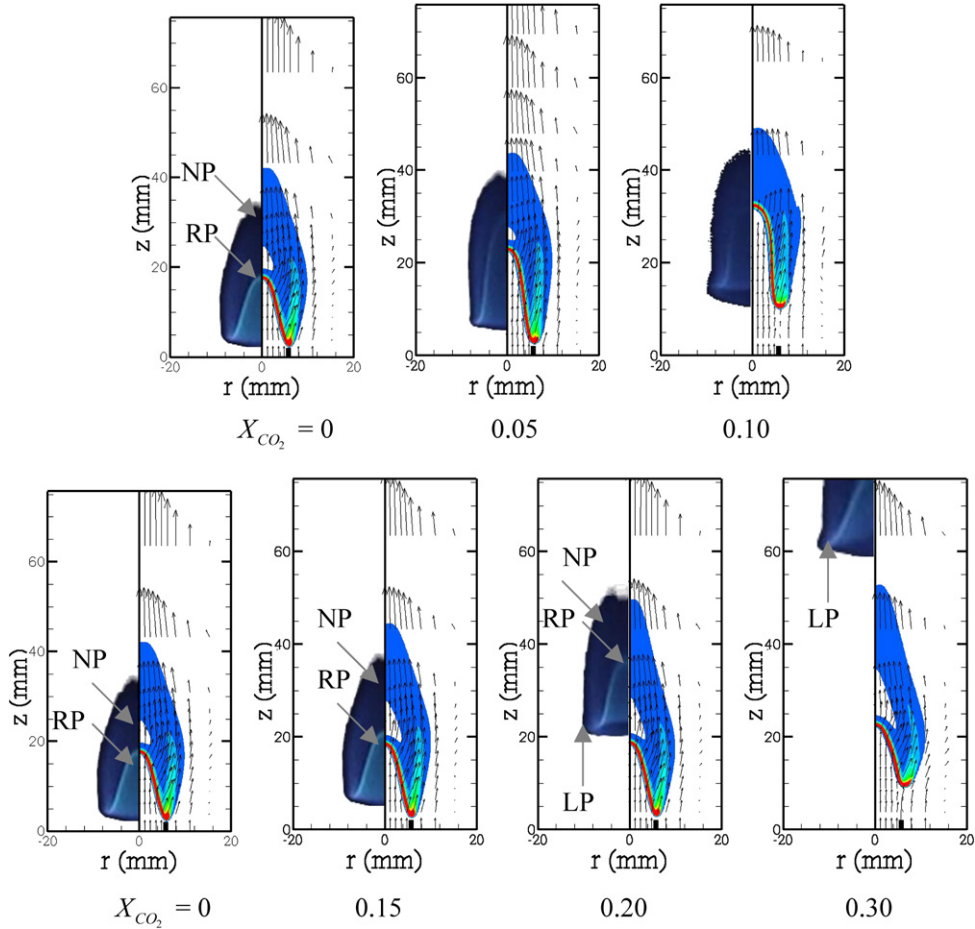


Fig. 2. Comparison of predicted heat-release-rate contours (right) with measured luminosity contours (left) for fuel-stream (top)- and air-stream (bottom)-diluted PPFs established at $\phi = 1.5$. Velocity vectors are shown for the simulated flames. The three reaction zones, rich premixed (RP), nonpremixed (NP), and lean premixed (LP) reaction zones, are also indicated in the figure.

flames under near-lifting conditions. Recently, Katta et al. [26] accurately predicted the minimum diluent concentration for blowout of methane–air nonpremixed cup burner flames.

We provide additional validation by comparing the predicted heat release rate contours with the measured luminosity images for fuel-stream and air-stream CO_2 -diluted partially premixed flames established at $\phi = 1.5, 2.25$, and a nonpremixed flame ($\phi = \infty$). As shown in Figs. 2–4, the numerical model in general reproduces the measured flame topology including the locations of the various reaction zones and the liftoff height for both fuel-stream- and air-stream-diluted flames.¹ At low dilution, the PPFs ($\phi = 1.5$,

and 2.25; cf. Figs. 2 and 3) are burner-attached² [25], whereas the NPF (cf. Fig. 4) is lifted. These flames (PPFs and NPF), however, exhibit a double-flame structure, containing two reaction zones, namely the rich premixed (RP) and the nonpremixed reaction (NP) zones. Further increase in dilution increases the flame liftoff heights and the flame structure changes from double to triple,³ as reactant mixing is enhanced in the wake region above the burner rim, allowing entrainment of air into the fuel and vice versa. The blue

¹ More detailed discussion on the comparison between measurements and simulations is provided in the following section.

² Here, a burner-attached flame is one that exhibits non-negligible heat transfer to the burner rim, whereas a lifted flame is stabilized downstream of the burner in a low-velocity region with negligible heat transfer to the burner rim.

³ The triple flame contains a rich premixed zone (on the fuel side), a nonpremixed zone, and a lean premixed zone, which is indicated by “LP” in the diluted flames of Figs. 2–4.

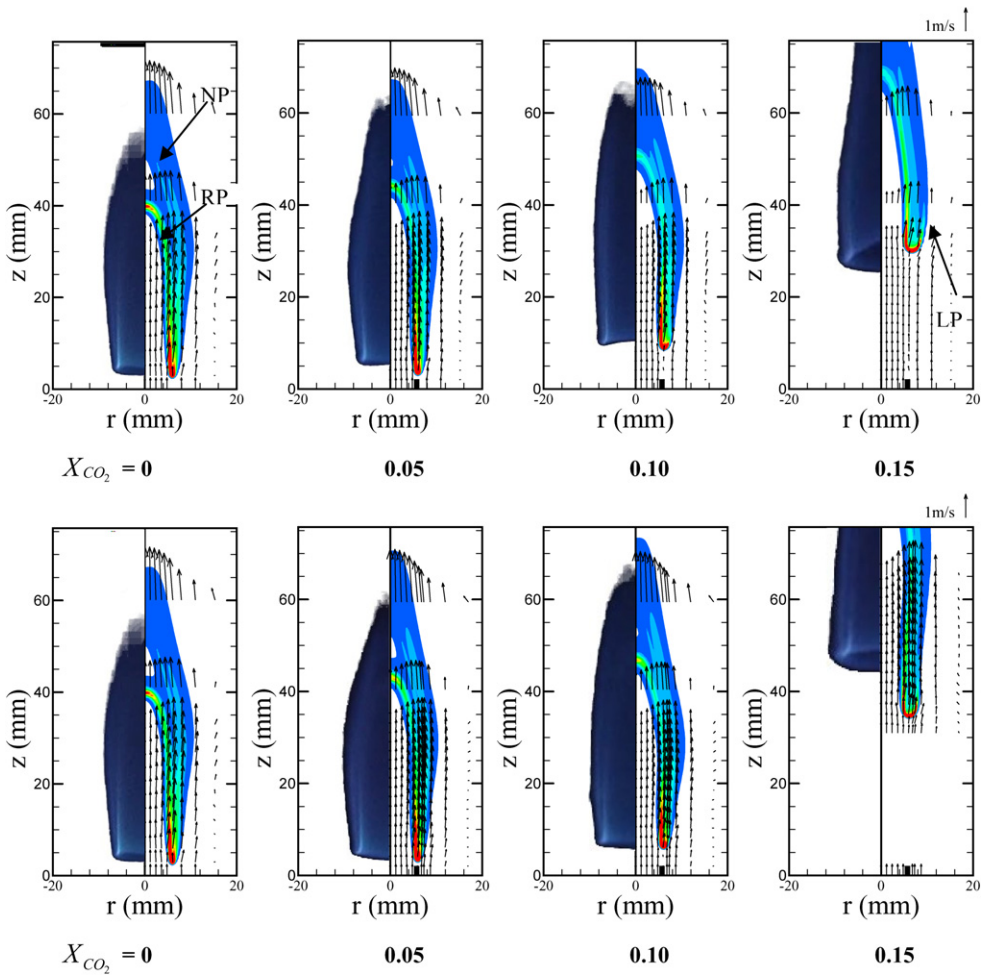


Fig. 3. Comparison of predicted heat-release-rate contours (right) with measured luminosity contours (left) for fuel-stream (top)- and air-stream (bottom)-diluted ($X_{CO_2} = 0.0, 0.05, 0.10, 0.15$), PPFs established at $\phi = 2.25$. Velocity vectors are shown for the simulated flames. The three reaction zones, rich premixed (RP), nonpremixed (NP), and lean premixed (LP) reaction zones, are also indicated in the figure.

color in all the experimental images represents the reaction zones, while the bright yellow in the NPFs corresponds to the soot incipience region. The flame luminosity is greatly diminished in the PPFs, indicating marked reduction in soot production due to partial premixing.

Both the simulations and the measurements indicate that flames exhibit well-organized oscillations induced by buoyant acceleration and so care is taken in comparing any two flames at the same phase angle. In the NPF (cf. Fig. 4), the buoyant acceleration of hot gases outside the flame surface causes shear-layer rollup, leading to the formation of a toroidal vortex that interacts with the flame surface at locations downstream of the flame base. On the other hand, the PPFs (cf. Figs. 2 and 3) do not indicate this toroidal vortex ring; instead, the flame pinches off when the

flame tip reaches its maximum amplitude. As noted earlier, the shape of the blue region in experimental images indicates the reaction zones. For instance, the undiluted PPF established at $\phi = 1.5$ exhibits two well-defined reaction zones (rich premixed and nonpremixed), as indicated in Fig. 2. As diluent is added to the fuel stream, the rich premixed zone becomes weaker and moves closer to the nonpremixed reaction zone, as indicated by its decreased luminous intensity and the decreased spatial distance between the two reaction zones (cf. Fig. 2). This effect is less pronounced when this flame is air-stream-diluted. This effect will be further examined in a later section.

The effect of fuel-stream and air-stream dilution on the flame liftoff height strongly depends on the level of partial premixing. Both measurements and simulations indicate that the liftoff height of the NPF

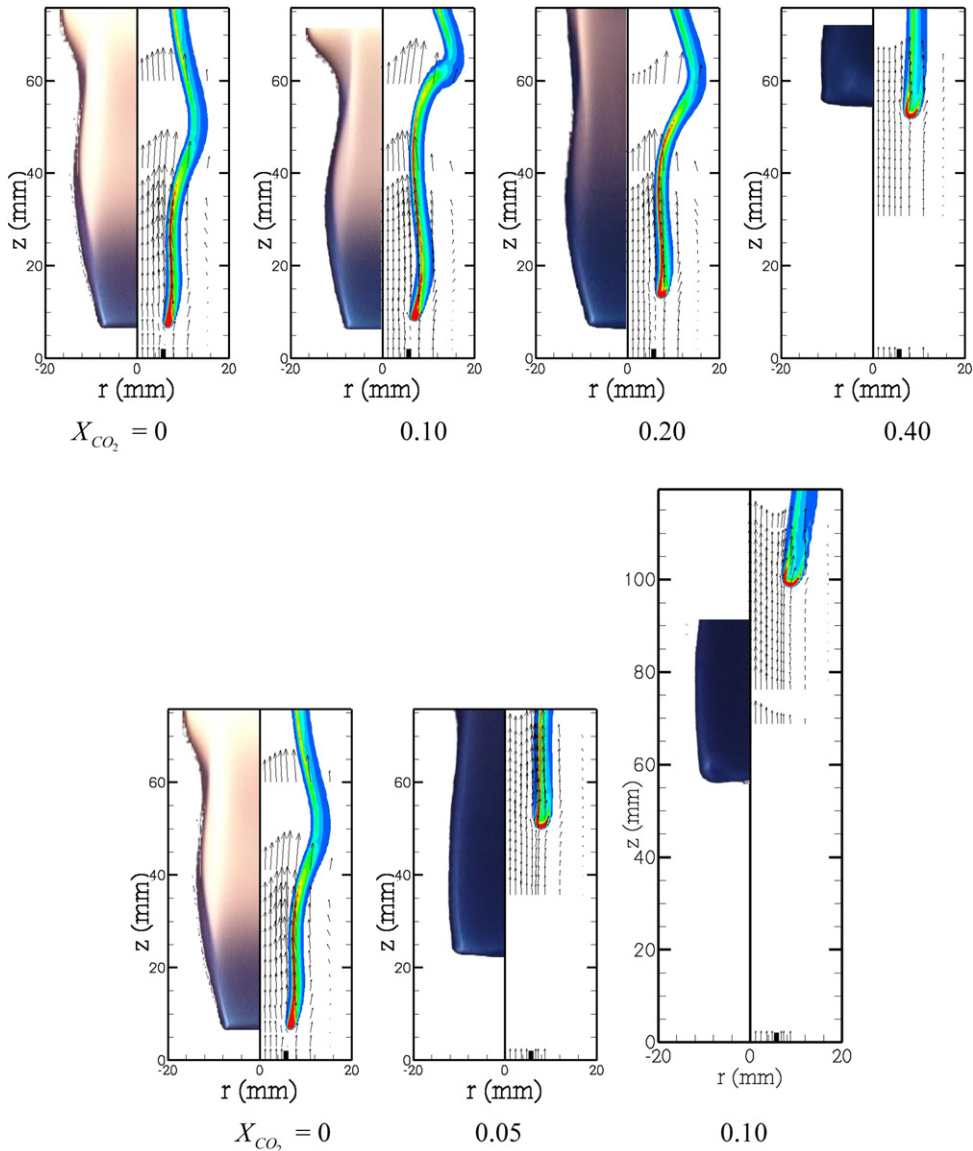


Fig. 4. Comparison of predicted heat-release-rate contours (right) with measured luminosity contours (left) for fuel-stream (top)- and air-stream (bottom)-diluted NPFs ($\phi = \infty$). Velocity vectors are shown for the simulated flames. The three reaction zones, rich premixed (RP), nonpremixed (NP), and lean premixed (LP) reaction zones, are also indicated in the figure.

is more sensitive to air-stream dilution (cf. Fig. 4), whereas the liftoff height of the PPF established at $\phi = 1.5$ is more sensitive to fuel-stream dilution (cf. Fig. 2). For example, the PPF established at $\phi = 1.5$ remains in a burner-attached mode even when air-stream dilution is $X_{\text{CO}_2} = 0.15$, while it is lifted when fuel-stream dilution is only $X_{\text{CO}_2} = 0.10$. In contrast, the liftoff height of the NPF remains relatively unchanged even when the fuel-stream dilution is $X_{\text{CO}_2} = 0.20$, but it increases dramatically when the air-stream dilution is only $X_{\text{CO}_2} = 0.05$.

The PPF established at $\phi = 2.25$, however, is only slightly more sensitive to fuel-stream dilution than to air-stream dilution. Therefore, as the level of partial premixing increases (i.e., ϕ decreases) the flame liftoff height becomes more sensitive to fuel-stream dilution than to air-stream dilution, and the transition for becoming more sensitive to fuel-stream dilution than to air-stream dilution seems to occur near $\phi = 2.0$. As discussed later, this transition can be related to the stoichiometric mixture fraction value.

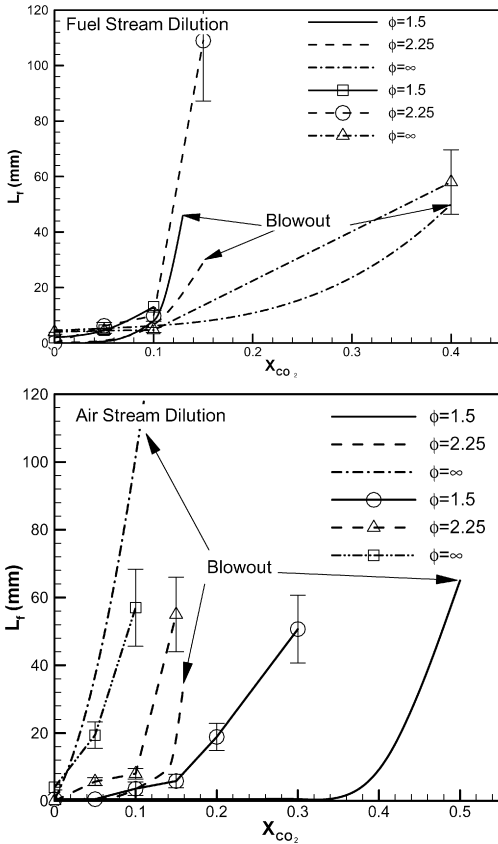


Fig. 5. Predicted (lines) and measured (lines with open and closed squares) liftoff height (L_f) plotted as a function of CO_2 mole fraction for the fuel (top) and air (bottom)-stream-diluted coflow PPFs (at $\phi = 1.5$ and 2.25) and NPF. The blowout conditions are also shown.

4.2. Flame liftoff and blowout (extinction) characteristics

Fig. 5 presents the measured and predicted liftoff heights plotted versus the amount of CO_2 dilution in the fuel stream (top) and air stream (bottom) for partially premixed ($\phi = 1.5, 2.25$) and nonpremixed ($\phi = \infty$) flames. The blowout conditions, in terms of the flame liftoff height and the critical CO_2 mole fraction at blowout, are also shown in the figure. Important observations from this figure are as follows.

1. There is generally good agreement between predictions and measurements in terms of the flame topology (cf. Figs. 2–4) and liftoff height at different dilution levels for both fuel-stream- and air-stream-diluted flames. The critical CO_2 mole fractions required for blowout (extinction) of PPFs and NPFs are also accurately predicted. The quantitative agreement between the measured and predicted liftoff heights is reasonable

at lower liftoff heights, but deteriorates near blowout conditions, which can be anticipated as the flames become more unsteady and quite sensitive to CO_2 dilution level just prior to blowout. In addition, the quantitative differences can be attributed to (i) uncertainties in the liftoff height measurements near blowout, (ii) sensitivity of the liftoff height to small changes in CO_2 mole fraction near blowout, (iii) sensitivity of the liftoff height to inflow boundary conditions and the geometric characteristics of the isothermal insert [19], and (iv) uncertainties in the chemistry and transport models used in simulations, especially near limit conditions.

2. Both the measurements and simulations indicate that the undiluted NPF is lifted and stabilized downstream of the burner rim, while the undiluted PPFs are stabilized at the burner rim. With fuel-stream dilution, the liftoff height of the NPF increases first gradually and then more rapidly until blowout occurs (cf. Fig. 5a). In contrast, the PPFs ($\phi = 1.5$ and 2.25) first lift off from the burner rim due to local extinction caused by dilution [25], which reduces heat transfer to the rim and the rate of H-atom destruction. Once these flames are lifted, their lift off heights increase much more rapidly than that of the NPF. Consequently, their liftoff heights exceed that of the NPF, and the diluent mole fractions required for their extinction (through blowout) are significantly smaller than those required for the extinction of NPF. In contrast, with air-stream dilution, the NPF lifts off rather rapidly from the burner (cf. Fig. 4) and blows out when a relatively small amount of CO_2 is added to the air stream (cf. Fig. 5b), while the PPFs lift off more slowly and blow out at a much higher CO_2 concentration.
3. The variation of liftoff height with CO_2 mole fraction as well as the critical CO_2 mole fraction at blowout depends strongly on the level of partial premixing and whether the CO_2 is added to the fuel stream or air stream. For fuel-stream dilution, the critical CO_2 mole fraction required for extinction increases as ϕ is increased (i.e., the level of partial premixing is decreased), while for air-stream dilution, the critical CO_2 mole fraction decreases as ϕ is increased. For the results presented in Fig. 5a, the predicted fuel stream CO_2 dilutions required for flame blowout at $\phi = 1.5, 2.25$, and ∞ are $X_{\text{CO}_2} = 0.12, 0.16$, and 0.41, respectively, and the corresponding measured values are $X_{\text{CO}_2} = 0.1, 0.15$, and 0.4. On the other hand, for air-stream dilution (cf. Fig. 5b), the predicted CO_2 dilutions required for flame blowout at $\phi = 1.5, 2.25$, and ∞ are $X_{\text{CO}_2} = 0.5, 0.18$, and 0.12, respectively, and

the corresponding measured mole fractions are $X_{\text{CO}_2} = 0.3, 0.15,$ and 0.1 . Thus, an important result from Fig. 5 is that NPFs are more difficult to extinguish than PPFs when the inert agent is added to the fuel stream, whereas PPFs are more difficult to extinguish when the agent is added to the air stream.

- Both the simulations and the measurements also indicate an intermediate level of partial premixing at which the air-stream and fuel-stream dilutions become equally effective in causing the flame liftoff and blowout. For the results presented in Fig. 5, this seems to occur at $\phi \approx 2.0$. Thus, for $\phi < 2.0$, the fuel-stream dilution is more effective, while for $\phi > 2.0$, the air-stream dilution is more effective in extinguishing the flame. As discussed later based on counterflow flame results, this crossover ϕ value is determined by the stoichiometric mixture fraction value.

4.3. State relationships for undiluted coflow and counterflow flames

In order to examine the similarity between the structure and extinction characteristics of CO_2 -diluted coflow and counterflow flames, we present in Fig. 6 the state relationships in terms of the profiles of major reactants species (CH_4 and O_2), major product species (H_2O and CO_2), and “intermediate” fuel species (H_2 and CO) with respect to the mixture fraction. Following Bilger [32], the mixture fraction (f) is defined as

$$f = \left(\frac{2Z_C}{W_C} + \frac{1}{2} \cdot \frac{Z_H}{W_H} + \frac{Z_{\text{O},2} - Z_{\text{O}}}{W_{\text{O}}} \right) \times \left(\frac{2Z_{\text{C},1}}{W_C} + \frac{1}{2} \cdot \frac{Z_{\text{H},1}}{W_H} + \frac{Z_{\text{O},2} - Z_{\text{O},1}}{W_{\text{O}}} \right)^{-1}, \quad (2)$$

where Z_i denotes the mass fraction of an element i of atomic mass W_i , the subscripts C, H, and O refer to carbon, hydrogen, and oxygen, respectively, and the subscripts 1 and 2 refer to the fuel and oxygen reference states. The fuel side and air side are indicated by $f = 1$ and $f = 0$, respectively in Fig. 6. Scalar profiles for counterflow flames established at $\phi = 1.5, 2.25,$ and 10 and a global strain rate of 100 s^{-1} are compared with those for the corresponding coflow flames. The species profiles for coflow flames are taken at a radial cut 2 mm above the flame base. As stated earlier, an undiluted nonpremixed coflow flame is lifted from the burner (cf. Fig. 4), which causes ad-

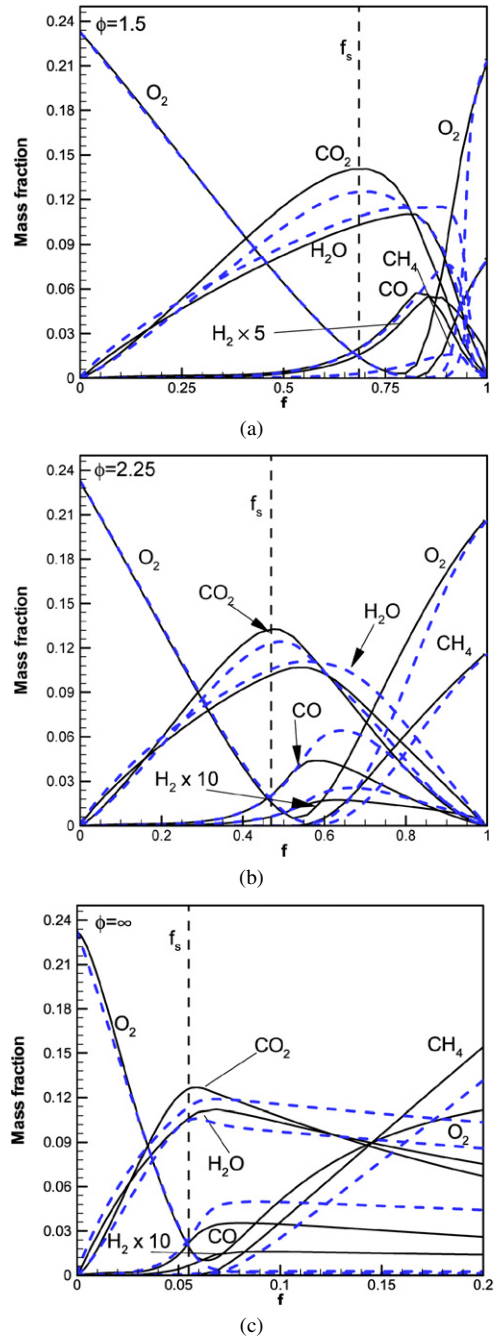


Fig. 6. State relationships in terms of scalar profiles plotted at an axial location of $z = (L_{\text{LE}} + 2) \text{ mm}$, where L_{LE} is the liftoff height, with respect to the mixture fraction (f) for the coflow PPFs (at (a) $\phi = 1.5$ and (b) 2.25) and (c) NPF ($\phi = \infty$). Analogous counterflow PPFs at $\phi = 1.5, 2.25,$ and 10 with a global strain rate of 100 s^{-1} are also shown for comparison with the corresponding coflow PPFs and NPF. The black (solid) and blue (dashed) lines represent results for the coflow and counterflow flames, respectively. The vertical dashed line represents the stoichiometric mixture fraction (f_s).

ditional mixing upstream of the flame,⁴ producing a nearly merged PPF structure at the flame base. Consequently, the corresponding counterflow flame is computed at an equivalence ratio of 10.

As discussed by Tanoff et al. [33] and Naha and Aggarwal [34], partially premixed combustion can be grouped into two distinct regimes, namely a double-flame and a merged-flame regime. In the first regime, a PPF contains two physically separated reaction zones, while in the second, the two reaction zones are nearly merged. Despite different configurations, there is good agreement in the scalar profiles of coflow and counterflow flames for the three cases presented in Fig. 6. Both the coflow and counterflow PPFs established at $\phi = 1.5$ exhibit a double-flame structure (cf. Fig. 6). The incoming CH₄ and O₂ from the fuel side are completely consumed in the rich premixed zone located near $f = 0.85$. The “intermediate” fuel species CO and H₂ are formed in the rich premixed zone and then transported and consumed in the non-premixed zone, which is located near $f = f_s$ (stoichiometric mixture fraction),⁵ and characterized by the peak CO₂ and H₂O values. The scalar profiles for PPF established at $\phi = 2.25$ and for NPF⁶ also exhibit similarity between the structures of coflow and counterflow flames. Both the counterflow and coflow flames exhibit a nearly merged partially premixed flame structure. In addition, for both counterflow and coflow flames, the consumption of major reactant species (CH₄ and O₂) in the rich premixed zone and that of major intermediate fuel species (CO and H₂) in the nonpremixed zone occur at nearly the same locations in the mixture fraction coordinate. The similarity between the steady counterflow and unsteady coflow partially premixed flames using the mixture fraction coordinate has also been observed by Aggarwal and Puri [35].

The results in Fig. 6 further indicate that as the level of partial premixing decreases (i.e., ϕ increases from 1.5 to ∞), the stoichiometric mixture fraction decreases from $f_s = 0.68$ to 0.055 and the rich premixed zone moves from the fuel side toward the air side. Note that the smaller f_s value for NPFs implies that more mixing is required to establish these flames compared to that for PPFs. Since mixture fraction is the ratio of the mass of material originating from the fuel stream to the total mass, the stoichiometric

mixture fraction (f_s) indicates whether the flame is located in a region of high or low concentration of material originating from the fuel stream. For $f_s > 0.5$, there is a higher concentration of material from the fuel stream, suggesting that the flame requires more reactant from the fuel stream; hence, fuel is the deficient reactant. Likewise, for $f_s < 0.5$, the flame is located in a region having a higher concentration of material from the air stream, suggesting that the flame requires more material from the air stream than from the fuel stream; hence, oxygen is the deficient reactant. As discussed in the next section, the stoichiometric mixture fraction plays an important role in characterizing the relative effectiveness of fuel-stream and air-stream dilution in extinguishing the flame for a given ϕ value.

4.4. Extinction characteristics of coflow and counterflow flames

Flame liftoff and blowout are complex processes involving transport, partial premixing, flame propagation, scalar dissipation, and extinction [36]. Nevertheless, results presented in the preceding section suggest that based on the observed similarity between the structures of coflow and counterflow flames, we can employ counterflow flame simulations to explain why fuel-stream dilution becomes more effective in causing flame extinction as the level of partial premixing is increased, and vice versa. Moreover, since counterflow flames have been extensively used previously to investigate strain-induced flame extinction [2,6], our results focusing on the dilution-induced extinction of such flames complement the previous results.

Fig. 7 presents the critical CO₂ mole fraction required for the extinction of fuel- and air-stream-diluted counterflow flames, plotted as a function of ϕ^{-1} (Fig. 7a) and f_s (Fig. 7b) for several global strain rates (a_s). The blowout conditions, in terms of the critical CO₂ mole fraction, for coflow flames are also shown in the figure. As indicated in Fig. 7a, for both counterflow and coflow flames, the critical fuel-stream CO₂ mole fraction required for extinction increases as ϕ is increased or the level of partial premixing is decreased. Conversely, the critical air-stream CO₂ mole fraction required for the extinction of counterflow and coflow flames decreases as ϕ is increased. Thus, in spite of the difference in configurations, the effects of partial premixing and fuel- and air-stream dilutions on the extinction of counterflow and coflow flames are similar. Moreover, as indicated in Fig. 7, the critical CO₂ mole fraction for counterflow flame extinction decreases as the global strain rate is increased. This is to be expected, since the flow residence time decreases at higher strain rates while the radical losses from the flame increase. The net

⁴ This is indicated by a relatively high mass fraction of oxygen penetrating into the fuel side in Fig. 6c.

⁵ The mixture fraction f reaches stoichiometry when the reactants are completely consumed; therefore, $f_s = (Z_{O_2}/W_{O_2})/(2Z_{C_1}/W_C + 1/2 \cdot Z_{H_1}/W_H + (Z_{O_2} - Z_{O_1})/W_O)$.

⁶ Here NPF refers to the coflow nonpremixed flame as well as the counterflow PPFs established at $\phi = 10$.

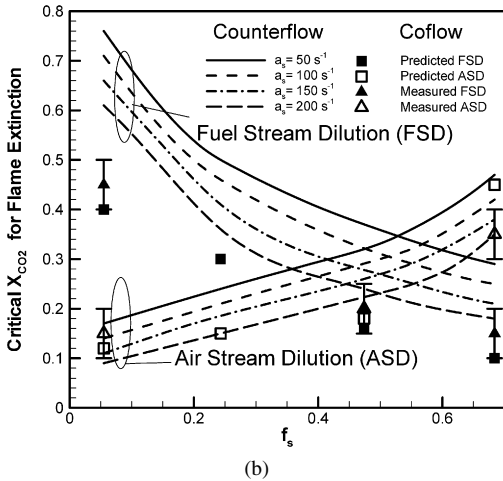
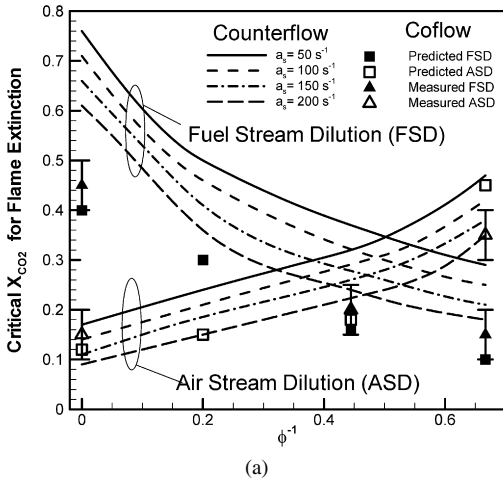


Fig. 7. Critical CO_2 mole fraction required for the extinction of fuel- and air-stream-diluted coflow and counterflow flames plotted as a function of (a) ϕ^{-1} and (b) f_s . The predicted and measured extinction conditions for fuel-stream (FSD)- and air-stream (ASD)-diluted coflow flames are represented by squares and triangles, respectively. Closed and open symbols represent, respectively, results for the fuel-stream- and air-stream-diluted coflow flames.

effect is that the flame temperature decreases, and, therefore, extinction is achieved with a lower diluent concentration for both fuel and air-stream-diluted flames.

Fig. 7 further shows that fuel- and air-stream dilutions are equally effective in flame extinction when the undiluted stoichiometric mixture fraction is $f_s \approx 0.5$ for both coflow and counterflow flames (regardless of the strain rate). For methane–air mixtures, $f_s \approx 0.5$ corresponds to an equivalence ratio of $\phi \approx 2.0$, and the mole fractions of CH_4 and O_2 are nearly equal (i.e., $X_{\text{CH}_4} = X_{\text{O}_2} = 0.1736$) so that the flame is located near the spatial center of the fuel and air streams. These results are consistent with

the scalar profiles discussed in the context of Fig. 6. Thus, an important observation from Figs. 6 and 7 is that $f_s = 0.5$ represents a crossover in characterizing the effectiveness of fuel-stream dilution versus air-stream dilution in extinguishing flames at various levels of partial premixing. Consequently, for flames with $f_s < 0.5$ (i.e., $\phi > 2.0$ for methane–air flames), oxygen is the deficient reactant, and, therefore, air-stream dilution is more effective in extinguishing these flames. In contrast, for flames with $f_s > 0.5$ (i.e., $\phi < 2.0$ for methane–air flames), fuel is the deficient reactant, and, thus, fuel-stream dilution is more effective in extinguishing these flames. Our results are in qualitative agreement with those reported by Seiser et al. [16], although, as previously discussed, their study focused on the strain-induced extinction of partially premixed flames.

The stoichiometric mixture fraction (f_s), while quite useful in characterizing the relative effectiveness of fuel-stream and air-stream dilution, does not indicate whether the diluent is extinguishing the flame through thermal or diluent effects. Since the maximum flame temperature (T_{max}) is a good indicator of the flame robustness, we can examine this aspect by monitoring the value of T_{max} as the diluent mole fraction in the fuel stream or air stream is increased. Fig. 8 plots T_{max} as a function of X_{CO_2} for counterflow partially premixed ($\phi = 1.5$) and nonpremixed flames at various global strain rates for both the fuel-stream and air-stream dilutions. As expected, as the amount of diluent increases in either the fuel or air stream, T_{max} decreases. In addition, the value of T_{max} at extinction decreases as the strain rate is increased, which can be attributed to the reduced residence time and the increased radical loss from the flame. More importantly, T_{max} decreases rapidly and almost linearly with increasing X_{CO_2} for the fuel-stream-diluted PPFs and air-stream-diluted NPFs. In contrast, the decrease of T_{max} with increasing X_{CO_2} is relatively slow but nonlinear for air-stream-diluted PPFs and fuel-stream-diluted NPFs. The flames exhibiting a linear T_{max} behavior with dilution extinguish at a much lower X_{CO_2} value as compared to flames exhibiting nonlinear behavior.

When a PPF is fuel-stream-diluted, T_{max} decreases linearly and rapidly because the diluent removes the deficient reactant (dilution effect) and cools the flame (thermal effect) effectively. Note that fuel is the deficient reactant for this case, per our discussion in the context of Figs. 6 and 7. In contrast, for air-stream dilution, the diluent no longer removes the deficient reactant (fuel), but only cools the flame (thermal effect). Since the deficient reactant for the NPF is oxygen, the opposite extinction behavior is observed in terms of fuel- and air-stream dilutions. Therefore, both thermal and dilution effects are present when

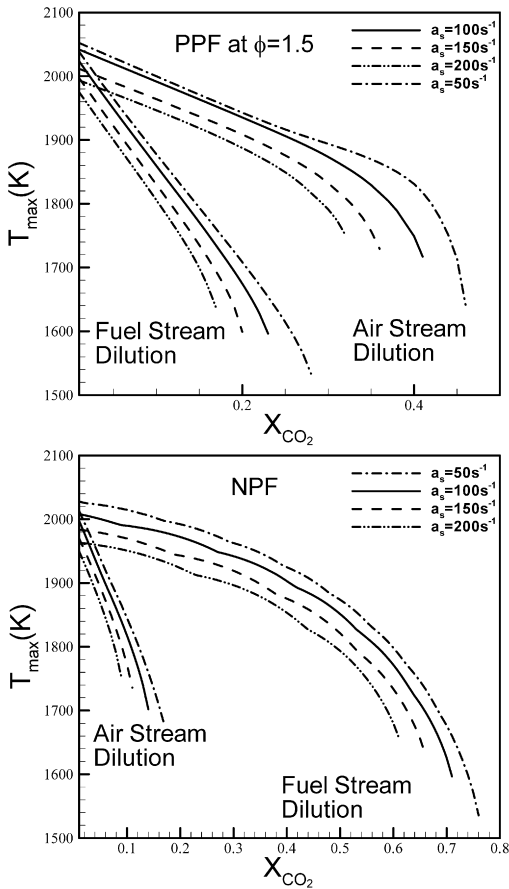


Fig. 8. Predicted maximum temperature as a function of CO_2 mole fraction at several global strain rates ($a_s = 50, 100, 150, 200 \text{ s}^{-1}$) for the fuel- and air-stream-diluted PPFs at $\phi = 1.5$ (top) and NPF (bottom).

extinguishing the fuel-stream-diluted PPF and air-stream-diluted NPF, while only the thermal effect is present when extinguishing the air-stream-diluted PPF and fuel-stream-diluted NPF. Consequently, a much higher diluent concentration is required for extinguishing the fuel-stream-diluted PPFs and the air-stream-diluted NPFs as compared to the requirements for extinguishing the air-stream-diluted PPFs and the fuel-stream-diluted NPFs.

5. Conclusions

An experimental and computational investigation has been performed to examine the extinction characteristics of partially premixed (PPF) and nonpremixed (NPF) flames in coflow and counterflow configurations using the chemically inert fire suppressant agent CO_2 . The major objectives is to characterize the relative effectiveness of fuel-stream dilution versus air-

stream dilution in extinguishing laminar methane–air flames established at various levels of partial pre-mixing. The similitude between the structure and extinction characteristics of air-stream and fuel-stream CO_2 -diluted coflow and counterflow flames has also been examined using the conserved scalar approach. Important observations are as follows:

1. There is generally good agreement between the measurements and predictions in terms of the topology of lifted flames, the liftoff heights, and the critical CO_2 mole fraction required for the blowout (extinction) of PPFs and NPFs. Both the measurements and predictions indicate that as the level of partial premixing increases (i.e., ϕ decreases) the flame liftoff height becomes more sensitive to fuel-stream dilution than to air-stream dilution. Consequently, as ϕ decreases, the fuel-stream dilution becomes more effective than the air-stream dilution in extinguishing the flame.
2. The state relationships in terms of the scalar profiles in mixture fraction coordinates exhibit remarkable similarity between the structures of coflow and counterflow flames. For both geometries, when the PPFs are fuel-stream diluted, the rich premixed reaction zone weakens, its flame speed decreases, and it moves closer to the non-premixed zone. Consequently, the reaction zones are nearly merged prior to blowout. Air-stream dilution has a less pronounced effect on the rich premixed zone than fuel-stream dilution.
3. Despite the difference in geometry, the extinction characteristics of CO_2 -diluted coflow and counterflow flames exhibit similarity. For both configurations, the critical CO_2 mole fraction at flame blowout depends strongly on the level of partial premixing and whether the diluent is added to the fuel stream or air stream. As ϕ is increased, the flame blowout occurs at higher CO_2 mole fraction for fuel-stream dilution, but at lower CO_2 mole fraction for air-stream dilution. Thus, NPFs are more difficult to extinguish than PPFs when the diluent is added to the fuel stream, whereas PPFs are more difficult to extinguish when the diluent is added to the air stream.
4. Both the simulations and experiments indicate an intermediate level of partial premixing at which the air-stream and fuel-stream dilutions become equally effective in causing the flame to lift off and blow out. For methane–air flames, this crossover seems to occur at a stoichiometric mixture fraction of $f_s = 0.5$, which corresponds to an equivalence ratio of $\phi \approx 2.0$. Thus, for $f_s > 0.5$, the fuel-stream dilution is more effective since fuel is the deficient reactant, while for $f_s < 0.5$,

the air-stream dilution is more effective in extinguishing the flame, since oxygen is the deficient reactant.

5. For fuel-stream-diluted flames with $f_s > 0.5$ and air-stream-diluted flames with $f_s < 0.5$, both thermal and dilution effects are present in extinguishing the flame. Consequently, these flames are more easily extinguished compared to the corresponding fuel-stream-diluted flames with $f_s < 0.5$ and air-stream-diluted flames with $f_s > 0.5$, since only thermal effects are present in extinguishing the latter flames.

Acknowledgments

This research was supported by the NASA Microgravity Research Division through Grant NCC3-688, for which Dr. Kurt Sacksteder serves as the technical monitor. Andrew Lock was supported by a fellowship through the NASA Graduate Student Research Program.

References

- [1] N. Peters, Proc. Combust. Inst. 20 (1984) 353–360.
- [2] K. Seshadri, I. Puri, N. Peters, Combust. Flame 61 (1985) 237–249.
- [3] H. Tsuji, Prog. Energy Combust. Sci. 8 (1982) 93–119.
- [4] A. Hamins, D. Trees, K. Seshadri, H. Chelliah, Combust. Flame 99 (1994) 221.
- [5] M. Bundy, A. Hamins, K.Y. Lee, Combust. Flame 133 (2003) 299–310.
- [6] D. Trees, A. Grudno, K. Seshadri, Combust. Sci. Technol. 124 (1997) 311–330.
- [7] N. Vahdat, Y. Zou, M. Collins, Fire Safe. J. 38 (2003) 553–567.
- [8] F. Liu, H. Guo, G.J. Smallwood, Ö.L. Gülder, Combust. Flame 125 (2001) 778–787.
- [9] UNEP, Montreal Protocol on Substances that Deplete the Ozone Layer, 2004.
- [10] C.M. Fleischmann, National Institute of Standards and Technology, USA, NIST-GCR-94-646, 1994.
- [11] C.M. Fleischmann, K.B. McGrattan, Fire Safe. J. 33 (1999) 21–34.
- [12] D.T. Gottuk, M.J. Peatross, J.P. Farley, F.W. Williams, Fire Safe. J. 33 (1999) 261–282.
- [13] W.G. Weng, W.C. Fan, L.Z. Yang, H. Song, Z.H. Deng, J. Qin, G.X. Liao, Combust. Flame 132 (2003) 709–714.
- [14] C.K. Law, G.M. Faeth, Prog. Energy Combust. Sci. 20 (1994) 65–113.
- [15] A.J. Lock, R. Ganguly, I.K. Puri, S.K. Aggarwal, U. Hedge, Proc. Combust. Inst. 30 (2004) 511–518.
- [16] R. Seiser, L. Truett, K. Seshadri, Proc. Combust. Inst. 29 (2002) 1551–1557.
- [17] A.J. Lock, A.M. Briones, X. Qin, S.K. Aggarwal, I.K. Puri, U. Hegde, Combust. Flame 143 (2005) 159–173.
- [18] Z. Shu, S.K. Aggarwal, V.R. Katta, I.K. Puri, Combust. Flame 111 (1997) 276.
- [19] R. Azzoni, S. Ratti, I.K. Puri, S.K. Aggarwal, Phys. Fluids 11 (1999) 3449.
- [20] X. Qin, I.K. Puri, S.K. Aggarwal, V.R. Katta, Phys. Fluids 16 (2004) 2963.
- [21] R. Siegel, J.R. Howell, Thermal Radiation Heat Transfer, Hemisphere Publishing Corporation, New York, 1981.
- [22] Z. Chen, X. Qin, B. Xu, Y. Ju, F. Liu, Proc. Combust. Inst. 31 (2007) 2693.
- [23] R.C. Reid, J.M. Prausnitz, B.E. Poling, The Properties of Gases and Liquids, McGraw–Hill, New York, 1987.
- [24] N. Peters, in: N. Peters, B. Rogg (Eds.), Reduced Kinetic Mechanisms for Applications in Combustion Systems, in: Lecture Notes in Physics, vol. 15, Springer, Berlin, 1993, pp. 3–14.
- [25] A. Briones, S.K. Aggarwal, V.R. Katta, Phys. Fluids 18 (2006) 043603.
- [26] V.R. Katta, F. Takahashi, G.T. Linteris, Combust. Flame 137 (2004) 506.
- [27] R.J. Kee, F.M. Rupley, J.A. Miller, M.E. Coltrin, J.F. Grcar, E. Meeks, H.K. Moffat, A.E. Lutz, G. Dixon-Lewis, M.D. Smooke, J. Warnatz, G.H. Evans, R.S. Larson, R.E. Mitchell, L.R. Petzold, W.C. Reynolds, M. Caracotsios, W.E. Stewart, P. Glarborg, C. Wang, C.L. McLellan, O. Adigun, W.G. Houf, C.P. Chou, S.F. Miller, P. Ho, P.D. Young, D.J. Young, CHEMKIN Release 4.0.2, Reaction Design, San Diego, CA, 2005.
- [28] M. Frenklach, C.T. Bowman, G.P. Smith, W.C. Gardiner, available at http://www.me.berkeley.edu/gri_mech/, Version 3.0, 1999.
- [29] V.R. Katta, T.R. Meyer, M.S. Brown, J.R. Gord, W.M. Roquemore, Combust. Flame 137 (2004) 198.
- [30] Z. Shu, B. Krass, C. Choi, S.K. Aggarwal, V. Katta, I.K. Puri, Proc. Combust. Inst. 27 (1998) 625.
- [31] F. Takahashi, W.J. Schmolli, V.R. Katta, Proc. Combust. Inst. 27 (1998) 675.
- [32] R.W. Bilger, Proc. Combust. Inst. 22 (1988) 475.
- [33] M.A. Tanoff, M.D. Smooke, R.J. Osborne, T.M. Brown, R.W. Pitz, Proc. Combust. Inst. 26 (1996) 1121.
- [34] S. Naha, S.K. Aggarwal, Combust. Flame 139 (2004) 90.
- [35] S.K. Aggarwal, I.K. Puri, AIAA J. 36 (1998) 1190.
- [36] N. Peters, F.A. Williams, AIAA J. 21 (1983) 423.